Colloid Polym Sci (2005) 283: 1137–1142
DOI 10.1007/s00396-005-1270-0

Y. Seto
T. Aoki
S. Kunugi

Temperature- and pressure-responsive properties of L- and DL-forms of poly(*N*-(1-hydroxymethyl)propylmethacrylamide) in aqueous solutions

Received: 16 August 2004
Accepted: 20 December 2004

Y. Seto · T. Aoki · S. Kunugi (✉)
Department of Polymer
Science and Engineering,
Kyoto Institute of Technology,
Matsugasaki, Sakyo,
Kyoto 606-8585, Japan
E-mail: kunugi@kit.ac.jp
Tel.: +81-75-7247836
Fax: +81-75-7247800

Abstract The structural transition of the L- and DL forms of poly(*N*-(1-hydroxymethyl)propylmethacrylamide (PHMPMA) in aqueous solution was studied by measuring the pressure dependence of the apparent scattering intensity, differential scanning calorimetry (DSC), and circular dichroism (CD). The thermodynamic implications of the results are discussed in relation to the chiral structure of the side chain, and differences in the thermal and barometric transitions. *T*-*P* diagrams of the transition showed characteristic ellipsoid features. Antagonism of the temperature and pressure effects was observed only for P(DL-HMPMA). For P(L-HMPMA), the transition temperature (T_{tr}) decreased with increasing pressure, and the highest T_{tr} was observed at atmospheric pressure (0.1 MPa). For both polymers, the highest P_{tr}s were observed at the lowest temperatures. The L polymer showed a specific negative peak in its CD spectrum at around 220 nm in the lower temperature region and the temperature dependence was reproduced by a single-step transition, with the midpoint corresponding to the T_{tr} obtained from the scattering measurements. Coupled with the results from the DSC, the different behavior between the P(L-HMPMA) and P(DL-HMPMA) could be explained in terms of the chain states before and after the transition. The cooperative factors derived from the DSC measurement revealed that about 4 to 5 polymers of the present size were necessary to perform a thermal transition for P(L-HMPMA), and that P(DL-HMPMA) underwent its transition as an almost single molecular event.

Keywords Poly(*N*-(L)-(1-hydroxymethyl)propylmethacrylamide) · Chiral polymer · Cloud point · Thermoresponsive polymer · High pressure

Introduction

Several synthetic polymers, including vinyl polymers, are known to show distinct changes in their molecular level states in solution in response to temperature. Poly(*N*-isopropylacrylamide) (PNIPAM) and other poly(acrylamide) derivatives with both hydrogen-bonded and hydrophobic interactions in aqueous solutions are some of the best-known examples [1–5]. These polymers show reversibly sharp transitions from their coiled to globular states upon an increase in temperature; this is termed inverse temperature transition. The swelling and shrinking of hydrogels prepared from such polymers have been studied experimentally and theoretically [3, 4]. These changes recall the behavior of proteins. PNIPAM can be considered as a simple but relevant protein model. The thermodynamic properties have been investigated from such a point of view, especially as a model for cold denaturation, since the coil to collapsed transition with increasing temperature is analogous to a transition from the unfolded to the folded structures of a protein across its cold renaturation temperature [6–8].

Besides temperatures, these thermoresponsive polymers can undergo structural transitions by changing pressures as well as soluble chemicals such as salts, surfactants, saccharides, and solvents [9–12]. Proteins also change their structures following exposure to extremely high pressures, with the critical value of the pressure being dependent on the nature and structure of the protein. We have investigated pressure-induced structural changes in proteins, polypeptides, and thermoresponsive synthetic polymers such as PNIPAM and poly(*N*-vinylisobutyramide) (PNVIBA) [13–19].

On the other hand, the introduction of an optically active property into a synthetic polymer seems to be essential to investigate the structural transition of the polymer into a protein model, and several attempts have been reported on some chiral polymers [20–24]. Recently, Aoki et al. synthesized an optically active poly(methacrylamide) derivative, poly(*N*-(L)-(1-hydroxymethyl)propylmethacrylamide) [P(L-HMPMA)], which has an asymmetric carbon in the side chain, and compared its thermoresponsive properties with the corresponding optically inactive P(DL-HMPMA), which was constructed with racemates of monomers [25, 26]. The aggregated state and structural transition of the optically active polymer were different from those of the racemic one, while these polymers showed their thermosensitivities in water.

In this report, we have measured the pressure dependence of the thermal transition for aqueous P(L-HMPMA) and P(DL-HMPMA) solutions, and discussed both the thermodynamic implications of the results with relation to the chiral structure of the side chain and the differences in the thermal and barometric transitions.

Materials and methods

P(L-HMPMA) and P(DL-HMPMA) were synthesized as previously reported [25]. Their weight-average molecular weights (M_w) and molecular weight distributions (M_w/M_n) were determined chromatographically (Shodex KF-806 column in DMF solution containing 0.1 w/v% LiCl, standardized against PEO). The M_ws were 58.7 kDa for P(L-HMPMA) and 66.8 kDa for P(DL-HMPMA). The molecular weight distributions of P(L-HMPMA) and P(DL-HMPMA) are 1.95 and 2.34, respectively. The $[\alpha]^{20}_{589}$ of P(L-HMPMA) was +33 °. Other chemical reagents were purchased from Nacalai Tesque (Kyoto, Japan) and Wako Pure Chemicals (Osaka, Japan).

In distilled water, P(L-HMPMA) and P(DL-HMPMA) are found to form solid precipitates and coacervates above their transition temperatures, respectively [25, 26]. The cloud points for the aqueous solutions of these polymers were determined by observing the apparent light scattering using a high-pressure optical cell constructed by Teramecs Co. (Kyoto, Japan) with three sapphire windows, embedded into a conventional fluorophotometer (Shimadzu, RF-5300PC), while tuning the excitation and emission light 400 nm. The experiments were performed by either scanning the temperature with an electronic regulator at constant pressure, or by scanning the pressure using a compact hand-driven high pressure pump at constant temperature. The heating and cooling rates of temperature were 0.5 °C/min and the exerting and releasing rates of pressure were approximately 0.1 MPa/s.

Circular dichroism (CD) spectrum was measured using a spectropolarimeter J-720 (Jasco, Tokyo, Japan). The quartz cell was thermostated using a circular water jacket equipped with a temperature controller (RTE-101, NESLAB, NH).

Differential scanning calorimetry (DSC) study was performed by a high-sensitivity DSC meter, Nano-DSC II Model 6100 (Calorimetry Science Co., UT, USA). About 0.3 ml of an aqueous polymer solution was introduced into the sample tube of the apparatus and the temperature-scanning rate was usually 1 K/min. The effects of the scanning rate on the obtained thermodynamic parameters were preliminary tested and checked.

Results and Discussion

Figure 1 shows the changes in the light scattering intensity of aqueous P(DL-HMPMA) solutions during temperature scanning (a; 0.5 °C/min), and during pressure scanning (b; ca. 0.1 MPa/s), at various fixed pressures and temperatures, respectively. The onset points, at which the intensity values became larger than zero in the temperature- and pressure-increasing measurements, were recorded as the apparent temperature or pressure of transition (T_{tr} or P_{tr}). These transitions were measured with both increasing scanning and decreasing scanning temperature or pressure. Examples of decreasing scanning are shown for 0.1 MPa (a) and 20 °C (b). Slight differences were observed between increasing and decreasing protocols, comparatively larger than those observed in the PNIPAM or PNVIBA solutions, but the processes seemed to be reversible.

Figure 2 shows the corresponding changes in the apparent light scattering of aqueous P(L-HMPMA) solutions responding to (a) temperature and (b) pressure changes at the indicated pressures and temperatures, respectively. There is significant hysteresis in the transition behavior against the heating and cooling cycle at

0.1 MPa, as shown in Fig. 2A. The observed hysteresis against temperature changes was in agreement with the previous report [25]. Above the transition temperatures, P(L-HMPMA) and P(DL-HMPMA) became solid precipitates and coacervates in hot water, respectively [26]. The precipitates by P(L-HMPMA) were stable to the extent that there was significant hysteresis in the phase separation of the aqueous polymer solution. In contrast to this, the pressure-induced changes of intensities exhibited very small hysteresis, for example, at 15.0 °C, and were in a manner similar to P(DL-HMPMA).

In Figs. 1 and 2, the onset points, at which the intensity values became larger than zero in the temperature- and pressure-increasing measurements, were de-

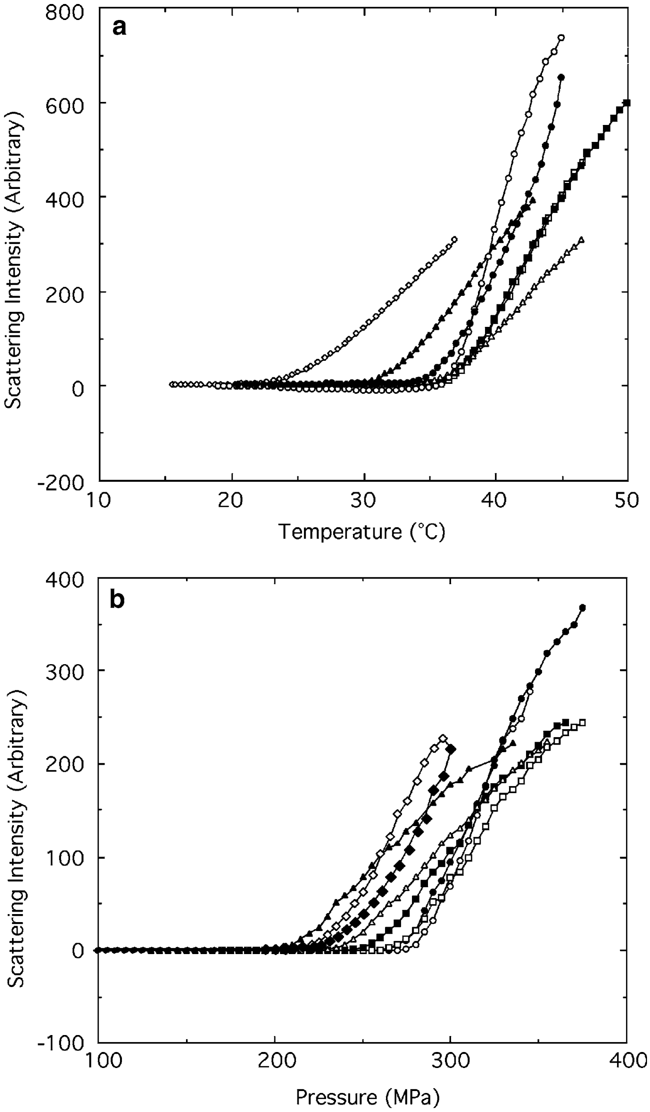

Fig. 1 Apparent light scattering change in aqueous P(DL-HMPMA) solution [0.1%(w/v)]. **a**: during temperature scanning. *open circle*, at 0.1 MPa (*T* increasing); *filled circle*, at 0.1 MPa (*T* decreasing); *open square*, at 50 MPa (*T* increasing); *filled square*, at 75 MPa (*T* increasing); *open triangle*, at 100 MPa (*T* increasing); *filled triangle*, at 150 MPa (*T* increasing); *open diamond*, at 200 MPa (*T* increasing). **b**: during pressure scanning. *open circle*, at −1.7 °C (*P* increasing); *filled circle*, at 2.3 °C; *open square*, at 8.9 °C (*P* increasing); *filled square*, at 13.0 °C (*P* increasing); *open triangle*, at 18.9 ° *C* (*P* increasing); *filled triangle*, at 24.7 °C (*P* increasing); *open diamond*, at 20.0 °C (*P* increasing); *filled diamond*, at 20.0 °C (*P* decreasing)

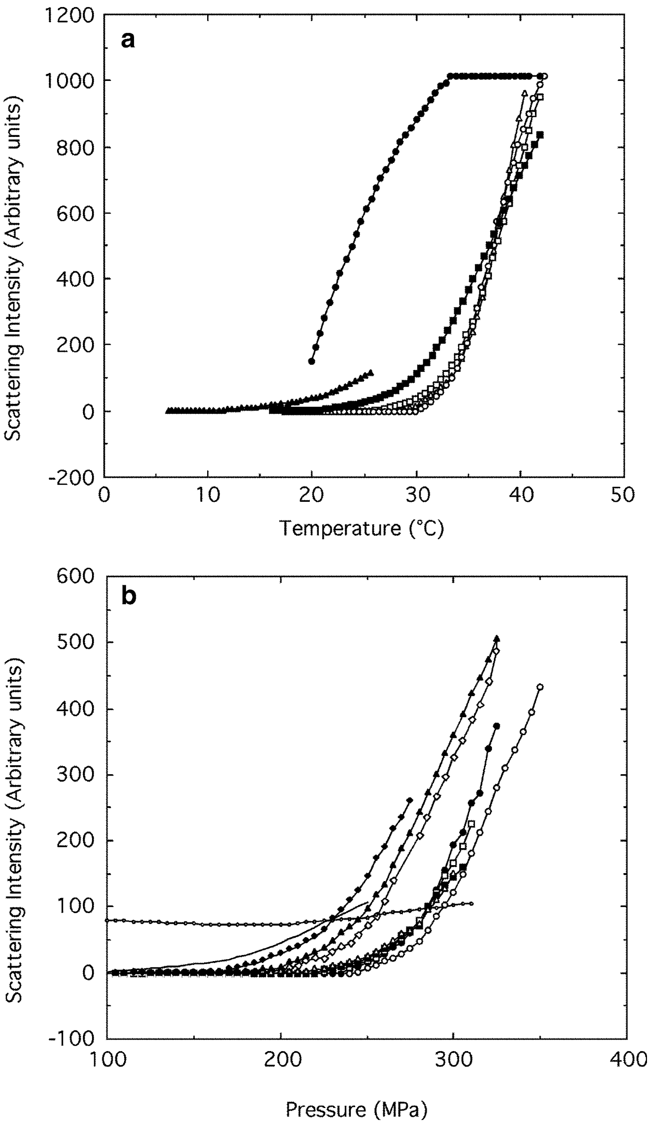

Fig. 2 Apparent light scattering change in aqueous P(L-HMPMA) solution [0.1%(w/v)]. **a**: during temperature scanning. *open circle*, at 0.1 MPa (*T* increasing); *filled circle*, at 0.1 MPa (*T* decreasing); *open square*, at 50 MPa (*T* increasing); *filled square*, at 150 MPa (*T* increasing); *open triangle*, at 200 MPa (*T* increasing). **b**: during pressure scanning. *open circle*, at −5.3 °C (*P* increasing); *filled circle*, at −2.0 °C (*P* increasing); *open square*, at 3.8 °C (*P* increasing); *filled square*, at 6.4 °C (*P* increasing); *open triangle*, at 10.7 °C (*P* increasing); *filled triangle*, at 15.0 °C (*P* increasing); *open diamond*, at 15.0 °C (*P* decreasing); *filled diamond*, at 20.0 °C (*P* increasing)

fined as the apparent temperature or pressure of transition (T_{tr} or P_{tr}). The T_{tr} and P_{tr} data were plotted to illustrate a *T*-*P* diagram, which was shown in Fig. 3. An overall shape of the diagram is either circular or elliptical [27]. The data obtained from *T*- and *P*-scanning measurements of aqueous P(DL-HMPMA) solution fitted one elliptical line, while the plots for P(L-HMPMA) have an increasingly downwards slope as the temperature is raised. Some synthetic polymers such as PNIPAM, PNVIBA, or others increased their transition temperatures with increasing pressure near atmospheric pressure and decreased with increasing pressure at pressures higher than 150–200 MPa. Unlike those polymers, P(DL-HMPMA) showed an elliptic line having a very small extremum at the low-pressure and high-temperature region, within the studied area of *T* and *P*. On the other hand, P(L-HMPMA) exhibited a circular line which decreased continuously with increasing temperature to give the highest T_{tr} at the atmospheric pressure of 0.1 MPa. For both polymers, the highest P_{tr}s were observed at the lowest temperatures within the studied area of *T* and *P*.

P(L-HMPMA) showed lower T_{tr} and P_{tr} than P(DL-HMPMA) at the same pressure and temperature, respectively. These polymers have different molecular weights (ca. 10% difference). A certain molecular weight dependence of the transition behavior was observed for PNIPAM and PNVIBA, but a difference of 10% in the *M*n would not be the reason for this difference in the diagrams; this can be reasonably explained in relation to the chiral properties of these polymers.

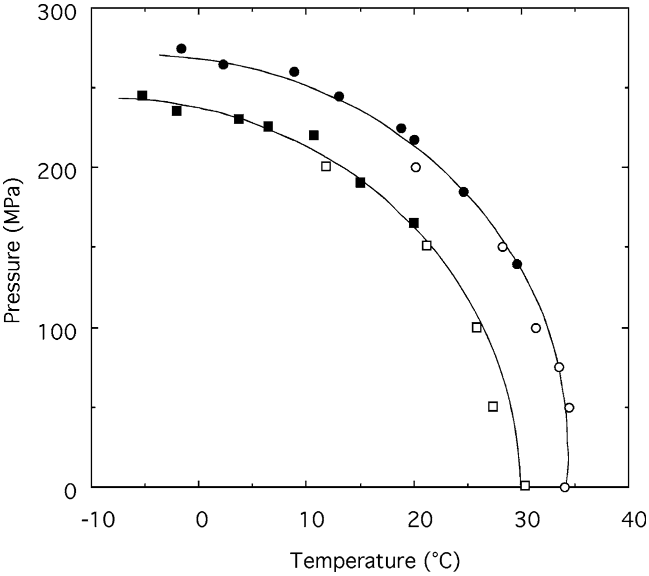

Fig. 3 *T*-*P* diagrams for the cloud points of aqueous PHMPMA solutions [0.1%(w/v)] in heating experiments. *open circle*, P(DL-HMPMA) *open square*, P(L-HMPMA). The open and closed symbols are for the *T*-scanning and *P*-scanning data, respectively

Since P(L-HMPMA) has a chiral center adjacent to the amide bond in the side chain, this polymer shows a specific CD spectrum as shown in Fig. 4A. The spectrum of soluble P(L-HMPMA) at low temperatures has a minimum at around 220 nm. With increasing temperature, this minimum became shallower, while the large and positive [θ] value at shorter wavelength decreased. The (negative) peak intensity at around 220 nm and the positive [θ] at around 205 nm were plotted against the temperature changes (Fig. 4B). At polymer concentrations of 0.1 w/v%, when the solution became turbid at higher temperatures, these profiles can be attributed to the turbidity, and can be reproduced by a single-step transition with midpoints of the main transitions well fitted to the T_{tr} from the scattering measurements. Even at lower concentrations of polymer (0.01%), where turbidimetric observations could barely be performed, some increase in the negative intensity at 225 nm was observed with increasing temperature (Fig. 4A inset and 4b), which indicates that some chiral structural changes would occur with increasing temperature. In addition, in the previous studies [26] and this study, the CD spectra of soluble P(L-HMPMA) exhibited large cotton effects, which implied a chiral amplification induced by a specifically formed structure. The structure must be based on interactions between the optically active chains.

The different behaviors between the present P(L-HMPMA) and P(DL-HMPMA) are related to the states before and after the transition. As explained before, the apparent solubility of P(DL-HMPMA) in water at low temperatures is higher than P(L-HMPMA). Water is a better solvent for P(DL-HMPMA). Transitions of these thermoresponsive polymers occur due to a dehydration process, and the strengthening of interactions among the side chains, as well as the structural deformation of water molecules around the hydrophobic groups. From a simple thermodynamic relationship of the transition, T_{tr} is described as $\Delta H(T_{tr})/\Delta S(T_{tr})$. The thermal transition is an endothermic process ($\Delta H(T_{tr}) > 0$) and thus $\Delta ST_{tr}) > 0$. A lower T_{tr} will correspond with either a smaller $\Delta H(T_{tr})$ or a larger $\Delta S(T_{tr})$. Actually, the DSC measurement revealed that the $\Delta H(T_{tr})$ and $\Delta S(T_{tr})$ values for P(DL-HMPMA) and P(L-HMPMA) were 2.3 kJ/monomer-mol and 7.4 J/K/monomer-mol and 0.9 kJ/monomer-mol and 2.9 J/K/monomer-mol, respectively, in very dilute solutions (0.05 w/v%). There existed some concentration dependences, and the thermodynamically determined T_{tr} was somehow lower than the turbidimetric ones shown above higher concentrations. The lower T_{tr} for the L form is dominated by the smaller $\Delta H(T_{tr})$, and this difference is substantially compensated by the smaller $\Delta S(T_{tr})$ of this form. The entropy change associated with this coil-globule transition comes mainly from the liberated water molecules. Solubility change of polymer (and thus the polymer conformation change) would give a negative entropy

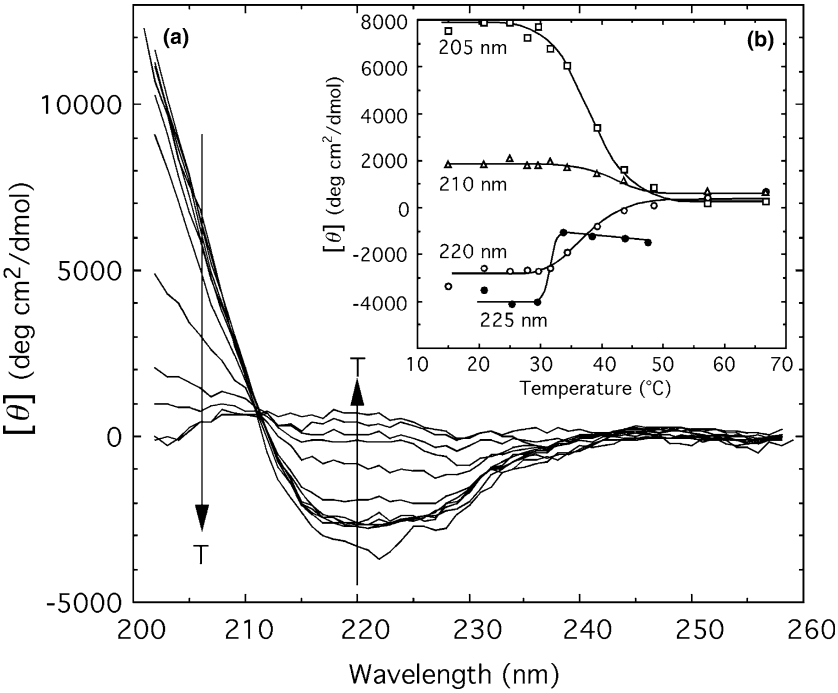

Fig. 4 Apparent CD spectra of aqueous P(L-HMPMA) solutions at various temperatures **a**, and the temperature dependence of [θ] at several wavelengths **b**. **a** [polymer] = 0.1%(w/v) in the main panel. *T*: 15.0, 20.8, 25.1, 27.9, 29.8, 31.7, 34.4, 39.2, 43.7, 48.5, 57.3, and 66.8 ° *C* along the arrow. **b**: *open square*, at 205 *nm*; *open triangle*, at 210 *nm*; *open circle*, at 220 *nm*. [polymer] = 0.1%(w/v). *filled circle*, at 225 *nm*. [polymer] = 0.01%(w/v)

change, which is overwhelmed by the positive entropy change generated from the liberated water.

It is notable that the cooperativity factor (*n*), as determined by the ratio of the van't Hoff enthalpy (ΔH^{vH}) and $\Delta H(T_{tr})$, was substantially different between these two forms. When this factor is described in terms of the number of cooperative monomeric units ($=\Delta H^{vH}/\Delta H(T_{tr})_{monomer}$), the factors are 450 and 1690 for P(DL-HMPMA) and P(L-HMPMA), respectively. This means that about 4 to 5 polymers of the present size are necessary to perform a thermal transition for P(L-HMPMA), whereas P(DL-HMPMA) can undergo the transition as an almost single molecular event. The dynamic light scattering (DLS) measurement in the previous study revealed that soluble P(L-HMPMA) showed a bimodal size distribution with diameters of approximately 12 and 90 nm, while soluble P(DL-HMPMA) had a single distribution with a diameter of 15 nm [25]. The optically active P(L-HMPMA) chains might be folded to form compact structures, and some compactly folded chains constituted a soluble associate with a diameter of 90 nm. P(DL-HMPMA) chains did not form the compact structure but favored to interact with water molecules. The DLS results might be closely related to the polymer numbers calculated from the above cooperativity factors for the thermal transitions of two P(HMPMA)s.

References

1. Scarpa JS, Mueller DD, Klotz IM (1967) J Am Chem Soc 89:6024
2. Heskins M, Guillet JE (1968) J Macromol Sci A2:1441
3. Tanaka T (1978) Phys Rev Lett 40:820
4. Shibayama M, Tanaka T (1993) Adv Polym Sci 109:1
5. Schild HG (1992) Prog Polym Sci 17:163
6. Tiktopulo EI, Bychkova VE, Ricka J, Ptitsyn OB (1994) Macromolecules 27:2879
7. Tiktopulo EI, Uversky VN, Lushchik BB, Klenin SI, Bychkova VE, Ptitsyn OB (1995) Macromolecules 28:7519
8. Kunugi S, Tanaka N (2002) Biochim Biophys Acta 1595:329
9. Bae YH, Okano T, Hsu R, Kim SW (1987) Makromol Chem Rapid Commun 8:481
10. Hoffman AS (1987) J Control Rel 6: 297
11. Gustafsson A, Wennerstrom H, Tjerneld F (1986) Fluid Phase Equilib 29: 365
12. Park TG., Hoffman AS (1993) Macromolecules 26: 5045
13. Kunugi S, Takano K, Tanaka N, Suwa K, Akashi M (1997) Macromolecules 30: 4499
14. Suwa K, Yamamoto K, Akashi M, Takano K, Tanaka N, Kunugi S (1998) Colloid Polymer Sci 276: 529
15. Kunugi S, Yamazaki Y, Takano K, Tanaka N, Akashi M (1999) Langmuir 15:4056
16. Kunugi S, Yamazaki Y, Tada T, Akashi M (2000) Langmuir 16:2042
17. Yamazaki Y, Tada T, Kunugi S (2000) Colloid Polym Sci 278:80

18. Yamaoka T, Tamura T, Seto Y, Tada T, Kunugi S, Tirrell AD (2003) Biomacromolecules 4:1680
19. Seto Y, Kameyama K, Tanaka N, Kunugi S, Yamamoto K, Akashi M (2003) Colloid Polym Sci 281:69020
20. Kulkarni RK, Morawetz H (1961) J Polym Sci 54:491
21. Braud C, Vert M (1978) Macromolecules 11:448
22. Moecellet-Sauvage J, Morcellet M, Loucheux C (1981) Makromol Chem 182:949
23. Yoshida M, Asano M, Kumakura M, Kataki R, Mashimo T, Yuasa H, Yamanaka H (1991) Drug Des Deliv 7:159
24. Aoki T, Nishimura T, Sanui K, Ogata N (1998) React Funct Polym 37:299
25. Aoki T, Muramatsu M, Torii T, Sanui K, Ogata N (2001) Macromolecules 34:3118
26. Aoki T, Muramatsu M, Nishina A, Sanui K, Ogata N (2004) Macromol Biosci 4:943
27. Hawley SA (1971) Biochemistry 10:2436